# Effects of Ligand Exchange Reactions on the Composition of $Cd_{1-y}Zn_yTe$ Grown by Metalorganic Vapor-Phase Epitaxy

**Menno J. Kappers, Kerri J. Wilkerson, and Robert F. Hicks***

*Department of Chemical Engineering, 5531 Boelter Hall, University of California at Los Angeles, Los Angeles, California 90095-1592*

*Received: January 3, 1997; In Final Form: March 14, 1997*[⊗]

The metalorganic vapor-phase epitaxy (MOVPE) of cadmium zinc telluride ($Cd_{1-y}Zn_yTe$) from dimethylcadmium (DMCd), dimethylzinc (DMZn), diethylzinc (DEZn), and diisopropyltelluride (DIPTe) was studied using on-line infrared spectroscopy to monitor the feed and effluent gases. The film composition was measured by X-ray diffraction. No zinc was incorporated into the film when DMCd and DMZn were used due to the very low reactivity of the latter compound. When DMCd and DEZn are tried, the films were nonuniform with Cd-rich films deposited at the reactor inlet and Zn-rich films deposited near the reactor outlet. This film profile was due to alkyl ligand exchange reactions between the group II precursors in the feed, producing DMZn, methylethylzinc (MEZn), methylethylcadmium (MECd), and diethylcadmium (DECd). The decomposition rates of these precursors vary over a wide range with DECd reacting at a 250 K lower temperature than DMZn. Since the organocadmium compounds were consumed at a much faster rate, CdTe was deposited first, while ZnTe was deposited downstream. The ligand exchange reactions explain why previous workers found it difficult to grow $Cd_{1-y}Zn_yTe$ alloys of uniform composition by MOVPE.

## Introduction

In the manufacture of large-area infrared focal plane arrays (IRFPAs), it is highly desirable to deposit the HgCdTe photodiodes directly onto GaAs (001) or sapphire (0001) substrates.[1−7] This is done in a two-step process, where $Cd_{1-y}Zn_yTe$ is first deposited on the GaAs or $Al_2O_3$ by vapor-phase epitaxy, and then $Hg_{1-x}Cd_xTe$ is deposited on the buffer layer by liquid-phase epitaxy. In order to minimize the number of defects in the film, the $Cd_{1-y}Zn_yTe$ buffer layer is lattice matched to the $Hg_{1-x}Cd_xTe$ active layer by incorporating between 4.1 and 3.6% zinc in the film. It is essential that the $Cd_{1-y}Zn_yTe$ alloy be highly uniform in composition, thickness, and crystallinity, as slight variations in the zinc content (>0.1%) can seriously impact the quality of the $Hg_{1-x}Cd_xTe$ epilayer. This makes composition control a critical issue.

Previously, Ahlgren et al.[8] and Kisker[9] have studied the MOVPE of $Cd_{1-y}Zn_yTe$ using DMCd, DEZn, and diethyltelluride (DETe) and compared the composition in the vapor-phase to the solid-phase composition. In Ahlgren's study, the deposition temperature was 714 K, and it was observed that the zinc preferentially incorporates into the film for all ratios of DMCd to DEZn in the gas inlet. Kisker studied the growth at lower temperatures and obtained very different results. At 653 K, zinc does not incorporate into the film below a group II vapor composition of 30% DEZn, and nearly pure ZnTe is deposited when the vapor composition exceeds 50% DEZn. This makes it very difficult to achieve a uniform zinc composition of only 4% over the entire substrate surface.

In a recent paper, Kappers et al.[10] proposed a kinetic model for alloy growth. This model assumes that the DEZn and DMCd compete for the same sites on the film surface and that, after desorption of the alkyl groups, the Cd and Zn atoms may either incorporate into the film or sublime off the surface. This model does fit Ahlgren's data but failed to fit Kisker's. At present, none of this previous work fully explains why the segregation of zinc in the film changes so dramatically with temperature.

In this study, on-line infrared spectroscopy was used to monitor the gas composition of the reactor feed and effluent during MOVPE of CdZnTe. It was discovered that exchange reactions occur between the alkyl ligands of DMCd and DEZn in the feed lines on the way to the reactor. This discovery explains the origin for the unusual alloy segregation behavior in II−VI MOVPE. The results of this study are described below.

## Experimental Section

The experimental apparatus and procedures used for this study have been described previously in detail.[11,12] An atmospheric-pressure MOVPE reactor was used to deposit $Cd_{1-y}Zn_yTe$ on the inner walls of a glass tube. The electronic-grade sources, DMCd, DMZn, DEZn, and DIPTe, were contained in 200 $cm^3$ stainless steel bubblers immersed in thermal regulating baths at 273, 258, 288, and 306 K, respectively. The precursors were vaporized into helium, which were then diluted further with helium or hydrogen to a total flow rate of 400−800 $cm^3\ min^{-1}$ and fed to the reactor. The carrier gases, He (99.995%) and $H_2$ (99.995%), were purified by deoxygenation traps and 13 X molecular sieves held at 196 K.

Using on-line infrared spectroscopy, the consumption rates of the organometallic compounds were determined.[12] Infrared spectra of the reactor feed and effluent were collected by passing the gas stream through a small flow cell, 17.7 cm long and 1.6 cm in diameter, and sealed with KBr windows. The data were acquired with a Digilab FTS-7 IR spectrometer, equipped with a wide-band MCT detector. The spectra shown herein were obtained by signal averaging 64 scans at 4 $cm^{-1}$ resolution. In Figure 1, the infrared spectra are shown of the gas feed and effluent from the reactor during $Cd_{1-y}Zn_yTe$ growth at 673 K from DMCd, DMZn, and DIPTe. The intense vibrational bands of the organometallic sources detected between 1600 and 450 $cm^{-1}$ are listed in Table 1 with the band assignments.[12−15] The

* To whom correspondence should be addressed.
[⊗] Abstract published in *Advance ACS Abstracts,* June 1, 1997.

S1089-5647(97)00062-X CCC: $14.00 

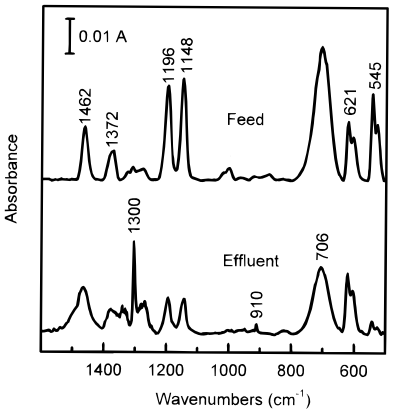


**Figure 1.** Infrared spectra of the reactor feed and effluent during $Cd_{1-y}Zn_yTe$ MOVPE with DMCd, DMZn, and DIPTe in hydrogen at 673 K, $4 \times 10^{-4}$ atm of DIPTe, a II/VI ratio of 1.0, an $x$ value of 0.3, and a total flow rate of 200 $cm^3$/min.

absorption bands are mostly well resolved from each other and provide a means of independently monitoring the consumption of each molecule during MOVPE.

Further inspection of Figure 1 reveals that the peak intensities of the organometallic compounds in the reactor effluent are much smaller than those of the feed and that additional sharp peaks appear in the spectrum of the effluent at 1300 and 910 $cm^{-1}$. These latter peaks correspond to the vibrational modes of the hydrocarbon products methane and propylene. Using the Beer's law, the intensities of the bands for the individual organometallic compounds can be converted into gas-phase concentrations to within 5% accuracy. The bands used are the metal−carbon stretching modes for DMCd, DMZn, and DEZn at 544, 621, and 572 $cm^{-1}$, respectively, and the intense skeletal mode for DIPTe at 1148 $cm^{-1}$. The corresponding molar absorption coefficients are $(57 \pm 5) \times 10^3$, $(76 \pm 2) \times 10^3$, $(57 \pm 2) \times 10^3$, and $(100 \pm 6) \times 10^3$ $cm^2$ $mol^{-1}$ for DMCd, DMZn, DEZn, and DIPTe.[12] The consumption rates of the precursors are determined during film deposition by monitoring the change in the peak intensity of the infrared bands from the inlet to the outlet of the reactor. Using the ideal gas law, the flux of the reactant in the feed is calculated from the total flow rate and the calibrated partial pressure of organometallic compound. The change in IR peak intensity between the feed and the effluent reflects the conversion of the reactant, and hence its consumption rate is known.

The films were analyzed using a $\theta/2\theta$ scan on a Crystal Logic powder diffractometer. The glass tube was sectioned into 1 cm pieces, which were split axially to reveal the film on the inner wall. Samples from the reaction zone of the tube were analyzed by scanning for the (111) and (331) peaks. The $2\theta$ ranges scanned were 22° to 26° and 61° to 68° by steps of 0.01°. Using Vegard's law and the measured peak position, the $Cd_{1-y}Zn_yTe$ film composition was calculated using[13]

$$y = \frac{a - a_{CdTe}}{a_{ZnTe} - a_{CdTe}} \quad (1)$$

where $a$ is the lattice constant (in angstroms) found by Bragg's law, $a_{ZnTe}$ is the lattice constant of ZnTe (6.1004 Å), and $a_{CdTe}$ is the lattice constant of CdTe (6.4823 Å). The peak position was taken to be the $2\theta$ corresponding to the maximum intensity value after the diffraction pattern was smoothed. The value of $y$ is calculated to within 5% error. In addition, the postdeposition region of the tubes was analyzed to determine whether cadmium or zinc metal was present. These samples were analyzed over a $2\theta$ range of 10°−100° by 0.1° steps.

The film thickness in each 1 cm section of the tube was also determined. The mass of the film was calculated from the difference in weight of the glass piece before and after etching it with a dilute bromine and methanol solution. Then the film area was obtained by multiplying the mass of the glass piece times the unit area per mass of the glass tube. Finally, the film thickness was calculated by dividing the film mass by its area and X-ray density. This method yielded about ±20% error in the thickness measurement. Film compositions averaged over the entire reactor were calculated by summing up the composition to weight ratio of each piece and multiplying this sum by the total film weight.

## Results

**Ligand Exchange.** Infrared spectroscopic analysis of a mixture of the group II precursors, DMCd and DEZn, reveals irregularities as compared to the individual compounds. Figure 2 shows the infrared spectrum of the mixture of DMCd and DEZn as a function of the initial feed composition, $x$, defined as

$$x = \frac{P_{DEZn}}{P_{DMCd} + P_{DEZn}} \quad (2)$$

where $P_{DMCd}$ and $P_{DEZn}$ are the partial pressure (in atmospheres) of DMCd and DEZn originally fed into the reactor. Surprisingly, the spectra in the figure do not show the expected summation of DMCd and DEZn absorption bands at different relative intensities. Instead, the DMCd and DEZn absorption

**TABLE 1: Assignment of the Infrared Bands Observed for the Organometallic Compounds between 1600 and 450 $cm^{-1}$ (Refs 12−15)[a]**

| DIPTe | | DMCd | | DMZn | | DEZn | |
|---|---|---|---|---|---|---|---|
| freq | assignt | freq | assignt | freq | assignt | freq | assignt |
| 504 (vw) | $\nu$(M−C) | 527 (s) | $\nu$(M−C) | 604 (s) | $\nu$(M−C) | 572 (s) | $\nu$(M−C) |
| 874 (vw), 923 (vw) | $\nu$(C−C−C) | 545 (s) | $\nu$(M−C) | 621 (s) | $\nu$(M−C) | 612 (br) | $\rho(CH_2)$ |
| 1000 (w) | $\rho(CH_3)$ | 709 (br) | $\rho$ ($CH_3$) | 706 (br) | $\rho(CH_3)$ | | |
| 1019 (vw), 1148 (s), 1197 (s) | $\nu$(C−C)/$\rho(CH_3)$ | | | | | 957 (vw), 986 (m), 1944 (vw) | $\nu$(C−C)/ ($CH_3$) |
| | | | | | | 1188 (w) | $\delta(CH_3)$ |
| | | | | | | 1234 vw) | $\omega(CH_2)$ |
| | | 993 (vw) | c/o | 1030(vw) | c/o | 1376 (sh) | c/o |
| 1303 (w), 1372 (m), 1462 (m) | $\delta(CH_3)$ | 1169 (vw), 1305 (w), 1327 (w) | $\delta(CH_3)$ | 1175 (vw), 1192 (w), 1304 (w) | $\delta(CH_3)$ | 1383 (m), 1421 (w), 1469 (w) | $\delta(CH_3)$ |

[a] Abbreviations: vw = very weak, w = weak, m = medium, s = strong, br = broad, sh = shoulder, c/o = combination/overtone.

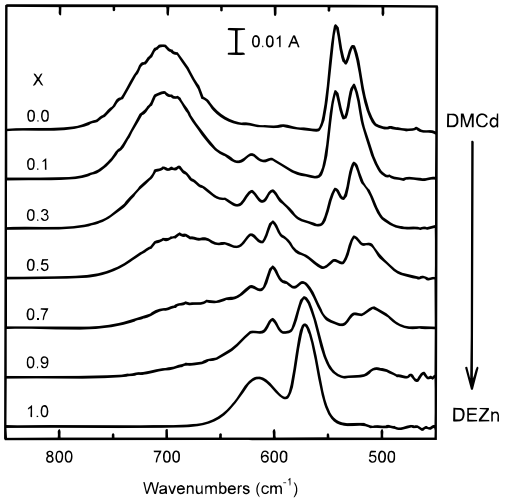


**Figure 2.** Infrared spectra between 850 and 450 $cm^{-1}$ of the group II organometallic compounds in the reactor feed during $Cd_{1-y}Zn_yTe$ MOVPE at varying ratios of DMCd to DEZn ($x = P_{DEZn}/(P_{DEZn} + P_{DMCd})$).

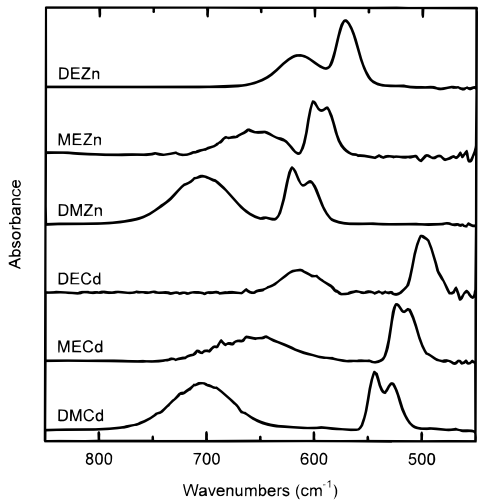


**Figure 3.** Infrared spectra between 850 and 450 $cm^{-1}$ of the group II organometallic compounds present after mixing DMCd and DEZn. All spectra are normalized to the same scale.

bands have decreased in intensity, and several new bands can be discerned in the spectra. The new bands show similar characteristics as those of DMCd and DEZn; hence, new organometallic compounds have been formed from the reaction of DMCd with DEZn.

Spectral subtraction reveals the absorption bands of four newly formed dialkyl species. By subtracting judiciously chosen IR spectra from each other, the infrared spectra of the different reaction mixtures can be deconvoluted into their components. The infrared spectrum of each organometallic compound is shown in Figure 3. One of the spectra is identical to that of DMZn. The infrared bands of another product agree well with those recorded previously for DECd.[13] However, no literature data are available for the other two species. These bands are assigned to the mixed alkyl compounds MECd and MEZn, since they are obvious products from the ligand exchange of DMCd and DEZn. Nevertheless, the infrared assignment for these species will be further justified below.

The spectra of DECd, MECd, and MEZn were obtained from those of the mixture as follows: The IR spectra of the compounds DMCd, DEZn, and DMZn were subtracted from the spectra shown in Figure 2, obtained after mixing DMCd and DEZn at the different ratios. At medium values of $x$ (0.30 $< x <$ 0.85) the residual IR spectrum represents a combination of the reaction products DECd, MECd, and MEZn. At higher and lower values of $x$, the residual spectrum contains only two of the three products, i.e., DECd and MEZn at $x > 0.85$ and MECd and MEZn at $x < 0.30$. The spectrum of MEZn was obtained by subtracting the DMZn spectrum from the IR spectrum of the reactor effluent at 625 K which contained only DMZn and MEZn (as described below). The spectrum of MEZn was used to obtain the IR spectra of DECd and MECd from those of the reaction mixtures at $x = 0.9$ and 0.1, respectively. The band positions in the spectral region between 800 and 450 $cm^{-1}$ and the proposed assignments for all components are summarized in Table 2.

**TABLE 2: Assignment of the Infrared Bands of the Organometallic Compounds between 1000 and 450 $cm^{-1}$**

| | peak position ($cm^{-1}$) of the organometallic compound | | | | | |
|---|---|---|---|---|---|---|
| assignt | DMZn | MEZn | DEZn | DMCd | MECd | DECd |
| $\nu_{M-C}$ | 604 | 589 | 572 | 523 | 512 | 504 |
| $\nu_{M-C}$ | 621 | 601 | | 544 | 525 | |
| $\delta_{CH_3}$ | 704 | 655 | 612 | 702 | 655 | 650 |

Next, the concentration of each organometallic compound was determined as a function of the initial feed composition, $x$. Since we were unable to calibrate the infrared band intensities of MEZn, MECd, and DECd, their concentrations were calculated as follows. Consider the reaction equilibrium

$$a\text{DMCd} + b\text{DEZn} \leftrightharpoons p\text{MECd} + q\text{MEZn} + r\text{DECd} + s\text{DMZn} \quad (3)$$

The values of $a$, $b$, and $s$ are determined from the intensities of the infrared bands and the corresponding molar absorption coefficients. In addition, the feed concentrations of DMCd and DEZn, $a_f$ and $b_f$, are known. A mass balance on the methyl ligands yields

$$2(a_f - a) = 2Aa_f = p + q + 2s \quad (4)$$

where $A$ is the conversion of DMCd. A mass balance on the ethyl ligands yields

$$2(b_f - b) = 2Bb_f = p + q + 2r \quad (5)$$

where $B$ is the conversion of DEZn. Mass balances on the Cd and Zn containing species give

$$a_f - a = Aa_f = p + r \quad (6)$$

$$b_f - b = Bb_f = q + s \quad (7)$$

The concentration of MEZn immediately follows after rewriting eq 7:

$$q = Bb_f - s \quad (8)$$

The concentration of DECd follows from the substitution of eqs 6 and 7 into eq 4:

$$r = Bb_f - Aa_f + s \quad (9)$$

After substitution of eq 9 into eq 6, the MECd quantity follows from

$$p = 2Aa_f - Bb_f - s \quad (10)$$

The exchange reactions may be assumed to be at equilibrium, since varying the flow rate has no effect on the gas-phase concentrations.

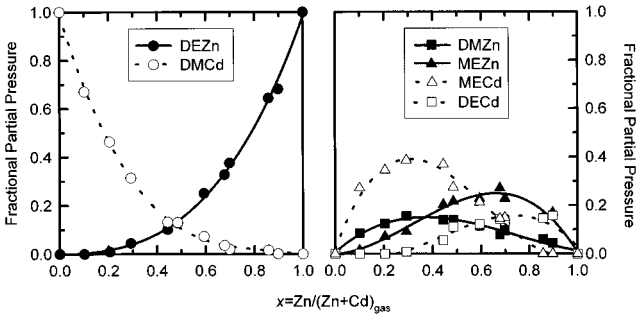


**Figure 4.** Fractional partial pressures of the group II organometallic compounds in the reactor feed during $Cd_{1-y}Zn_yTe$ MOVPE at varying $x$ values.

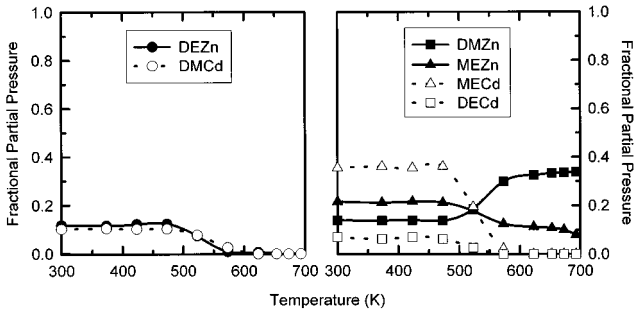


**Figure 5.** Fractional partial pressures of the group II organometallic compounds in the reactor effluent at varying temperatures for an $x$ value of 0.5.

Equations 3−10 have been used to calculate the partial pressures of MECd, DECd, and MEZn in the mixtures fed to the MOVPE reactor. The calculated values agree well with the trends in the infrared band intensities of these three compounds. Shown in Figure 4 is the dependence of the fractional partial pressure of each organometallic compound on the feed composition, $x$. The fractional partial pressure is taken to be the partial pressure of the species divided by the total partial pressure of all the group II species. On the left side are the curves obtained for DMCd and DEZn. As expected, the fractional partial pressure of DEZn increases as the value of $x$ increases, and the fractional partial pressure of DMCd decreases with increasing $x$. Both curves, however, are concave-up because their partial pressures in the mixture have decreased compared to those initially in the feed. The partial pressures of DMZn and MECd formed by the exchange reaction increase with $x$ and reach a maximum at $x = 0.3$. The amount of MECd formed is about twice that of DMZn at the maximum. The partial pressures of MEZn and DECd slowly increase with $x$ and attain their highest value at $x = 0.6$. Note that, at $x$ values higher than 0.6, the DMCd is almost completely converted into MECd and DECd.

Shown in Figure 5 is the dependence of the fractional partial pressures of the group II precursors in the reactor outlet on the reactor temperature for a zinc mole fraction in the feed gas of 0.5. On the left side of the figure, the fractional pressures of DMCd and DEZn are shown. On the right side, the products of the ligand exchange reaction, DMZn, MEZn, MECd, and DECd, are shown. The overall equilibrium does not change significantly between 300 and 470 K, leaving the partial pressures of each compound constant. However, the partial pressures of all the precursors, except DMZn, decrease above a temperature of 470 K. The sudden decrease in partial pressure of the reaction components is attributed to the decomposition of DECd, which starts at about 470 K. The original precursors, DMCd and DEZn, only start to decompose at 570 and 630 K, respectively. At 650 K, the Cd precursors and DEZn are completely decomposed, while MEZn and DMZn remain unaffected. The pyrolysis of MEZn and DMZn begins at 670 and 715 K, respectively. The shift toward more DMZn production at higher temperatures and the high thermal stability of the MEZn and the DMZn results in a low conversion of the organozinc compounds. At 700 K, only 11% of the zinc species in the feed is deposited, while all the organocadmium reactants are converted.

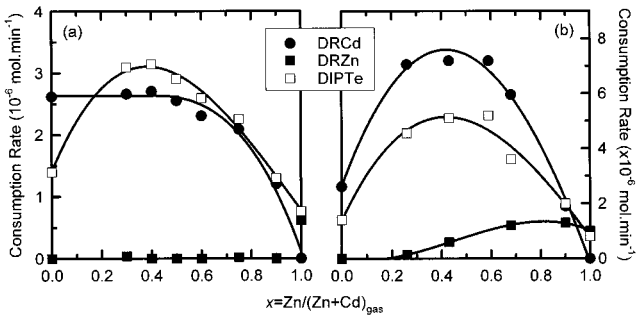


**Figure 6.** Dependence of the consumption rates of the organometallic compounds on the vapor composition during $Cd_{1-y}Zn_yTe$ MOVPE at 673 K and a II/VI ratio of 1.0: (a) DMCd, DMZn, and DIPTe; (b) DMCd, DEZn, and DIPTe.

In summary, the experiments verify that alkyl ligand exchange occurs between DMCd and DEZn in the gas phase. From the experiments conducted, there is no indication that the reaction could have occurred on the walls of the stainless steel tubing; the composition of the feed did not change with either the total flow rate or the temperature (<370 K) of the tubing leading to the IR cell. However, we cannot absolutely rule out that ligand exchange is catalyzed by the tube wall. Of the newly formed species in the feed, the DECd and MECd are much more reactive than DMZn and MEZn. The reactivity of the precursors increases in order: DMZn < MEZn < DEZn < DMCd < MECd < DECd.

**MOVPE of $Cd_{1-y}Zn_yTe$ Using DMZn.** Films of $Cd_{1-y}Zn_yTe$ were deposited using DMCd, DMZn, and DIPTe at temperatures between 673 and 748 K and at II/VI ratios of 1.0 and 2.0. In Figure 6a, the consumption rates of the organometallic compounds are plotted as a function of the feed composition during MOVPE at 673 K, a II/VI ratio of 1.0, and a DIPTe partial pressure of $4 \times 10^{-4}$ atm. The only precursors that are consumed are DMCd and DIPTe. The cadmium species consumed in excess of the DIPTe are deposited as a metal film or particulates in the reactor outlet.[11] In line with this, no zinc metal is deposited downstream. The zinc from DMZn is not incorporated into the film at any $x$ value other than 1.0, at which point pure ZnTe is grown.

During the growth of CdTe from DMCd and DIPTe ($x = 0$), the consumption rate of DMCd is greater than that of DIPTe for the reaction conditions selected. With decreasing partial pressure of DMCd, the consumption rate of DMCd remains constant, while that of DIPTe increases. The consumption rates cross each other between $x = 0.0$ and 0.3. A similar change of consumption rates with decreasing II/VI ratio has been observed before during CdTe OMVPE.[11] At $x$ values higher than 0.5, the consumption rates of DMCd and DIPTe both decrease as the zinc mole fraction in the feed increases. This latter trend is obviously due to the decline in the DMCd partial pressure.

**MOVPE of $Cd_{1-y}Zn_yTe$ Using DEZn.** Shown in Figure 6b are the consumption rates of DIPTe, all the cadmium sources (depicted as DRCd), and all the zinc sources (depicted as DRZn) during growth at 673 K, a DIPTe partial pressure of $1.1 \times 10^{-3}$ atm, and a II/VI ratio of 1.0. The combined consumption rate of the organocadmium compounds is higher in the mixture than

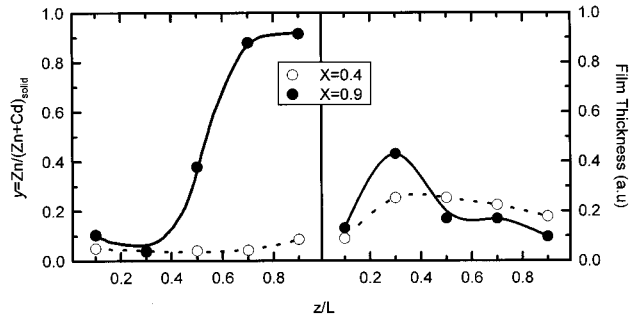


**Figure 7.** Dependence of the composition (left) and the thickness (right) of the film on the relative axial position in the reactor during $Cd_{1-y}Zn_yTe$ MOVPE with DMCd, DEZn, and DIPTe at 673 K, a II/VI ratio of 1.0, and $x$ values of 0.4 and 0.9.

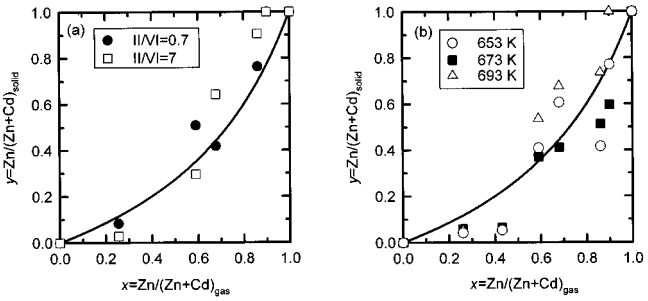


**Figure 8.** Composition of the solid versus the vapor for $Cd_{1-y}Zn_yTe$ MOVPE with DMCd, DEZn, and DIPTe for (a) II/VI ratios of 0.7 and 7.0 at 693 K and (b) growth temperatures of 653, 673, and 693 K at a II/VI ratio of 1.0. The solid curves are the result of calculations described in the text.

when DMCd reacts with DIPTe to form CdTe (i.e., compare $x = 0.3$ to $x = 0.0$). Moreover, the data points at $x > 0.5$ correspond to 100% conversion of the cadmium species. On the other hand, the combined consumption rate of the zinc species only slightly exceeds that of the DEZn during ZnTe MOVPE ($x = 1.0$). Once again, these results are indicative of ligand exchange reactions which produce less stable organocadmium compounds, MECd and DECd, relative to DMCd, and more stable organozinc compounds, MEZn and DMZn, relative to DEZn. The excess cadmium plates out as a metal film in the reactor outlet; no zinc metal is deposited downstream.

There is a distinct difference in the uniformity of the $Cd_{1-y}Zn_yTe$ film grown at low and high $x$ values. Figure 7 shows how the film composition (left) and the film thickness (right) changes down the length of the reactor tube for $x$ values of 0.4 and 0.9 and a growth temperature of 673 K. For $x = 0.4$, a fairly uniform film containing about 4% zinc is deposited throughout the heated zone. At the higher $x$ value, an alloy film containing 90% CdTe is deposited over the first 40% of the reactor, while a film of 90% ZnTe is deposited over the last 20% of the reactor. The film rich in CdTe at the inlet of the reactor is almost 4 times as thick as the film rich in ZnTe near the outlet. The transition from cadmium- to zinc-rich film growth occurs at a point where all the cadmium-containing species have been depleted from the gas phase. This point tends to shift toward the inlet with increasing growth temperature.

Shown in Figure 8 are zinc segregation curves determined from the weight-averaged composition of the films deposited in the reactor. The solid curves in the figures are the result of calculations to be described later in the text. The scatter of the data is particularly large at the higher values of $x$, due to the difficulties in obtaining accurate measurements of film composition and thickness down the length of the tube. Nevertheless, it is evident that the composition of the $Cd_{1-y}Zn_yTe$ film does not vary consistently with the II/VI ratio, or temperature, graphs a and b, respectively. A 10-fold increase in II/VI ratio and a 40 K increase in temperature have no significant effect upon the trends observed. It should be noted that the film compositions calculated from the infrared data produce segregation curves in reasonably good agreement with the results presented in the figure.

## Discussion

**Ligand Exchange.** The analysis of the feed gases by infrared spectroscopy reveals that the group II organometallic compounds undergo rapid exchange of their methyl and ethyl ligands during transport to the MOVPE reactor. Equilibrium between the reaction components is reached within the time scale of mixing in the feed lines and the IR gas cell (20 s). From the infrared spectra in Figures 2 and 3, four of the six reaction components can be readily identified, i.e., the two starting reactants, DMCd and DEZn, and their fully exchanged counterparts, DECd and DMZn. There is no precedent in the literature for the vibrational spectra of the two remaining zinc and cadmium species. However, the vibrational spectra of mixed alkyl complexes of lead,[16] germanium,[17] and arsenic[18,19] are well described. It was observed that the values of the metal−carbon stretching frequencies for the mixed alkyl species lie between the values of the fully exchanged alkyl species. For example, the average value of the degenerate Pb−C stretching frequency shifts gradually to lower values with each consecutive exchange of a methyl group for an ethyl group: from 469 $cm^{-1}$ for tetramethyllead, to 465 $cm^{-1}$ for trimethylethyllead, to 459 $cm^{-1}$ for dimethyldiethyllead, to 456 $cm^{-1}$ for methyltriethyllead, and to 452 $cm^{-1}$ for tetraethyllead.[16] The average values for the degenerate Cd−C and Zn−C stretching frequencies shift in an analogous fashion: from 534 $cm^{-1}$ for DMCd to 519 $cm^{-1}$ for MECd to 504 $cm^{-1}$ for DECd and from 613 $cm^{-1}$ for DMZn to 595 $cm^{-1}$ for MEZn to 572 $cm^{-1}$ for DEZn (from Table 2).

In total, 14 different alkyl ligand exchange reactions occur simultaneously in the mixture of DMZn, MEZn, DEZn, DMCd, MECd, and DECd. The reactions occurring between zinc and cadmium compounds with different ligands that lead to ligand exchange are listed in Table 3. The self-exchange reactions, of which there are six, and the exchange reactions of solely methyl, or ethyl ligands, of which there are two, have been omitted from this Table.

Ligand exchange between different group II organometallic compounds was investigated during the late 1960s. For instance, McCoy and Allred studied the reaction between DMCd and DMZn in solution by nuclear magnetic resonance.[20] The effect of the solvent on the reaction kinetics for methyl exchange between DMCd and DMZn and for interactions of DMCd with group III organometallic compounds were investigated by Oliver and co-workers.[21,22] It was found that these reactions proceed rapidly under mild conditions. The alkyl ligands transfer from one metal center to the other via a four-centered transition state:[21,22]

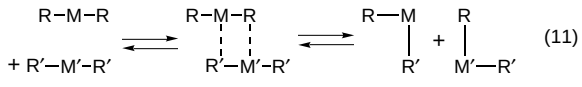


(11)

where R, R′ are $CH_3$ and/or $C_2H_5$ and M, M′ are Zn and/or Cd. To our knowledge, the reactions listed in Table 3 have never been studied before in the gas. We assume that the same mechanism and thermodynamics hold for the reactions in the gas as for those in solution. Recent $^1H$ NMR measurements on a 1:1 mixture of DMCd and DEZn in the liquid reveal that, to within the experimental error, the same ligand exchange products are formed at the same relative concentrations as that

**TABLE 3: Alkyl Ligand Exchange Reactions Observable by Infrared Spectroscopy**

| reaction | no. |
|---|---|
| DEZn + DMCd ⇌ MEZn + MECd | R1 |
| MEZn + MECd ⇌ DMZn + DECd | R2 |
| MEZn + DMCd ⇌ DMZn + MECd | R3 |
| DEZn + MECd ⇌ MEZn + DECd | R4 |
| DEZn + DMZn ⇌ 2MEZn | R5 |
| DMCd + DECd ⇌ 2MECd | R6 |

measured in the gas.[23] The standard heat of formation for DEZn and DMZn differs by 2 kcal/mol, while those for DECd and DMCd differ only by 0.1 kcal/mol.[24] Although the values are unknown for MECd and MEZn, the heat of formation for these species is expected to have a value close to the average of their dimethyl and diethyl counterparts. This suggests that the change in the free energy for the exchange reactions R1−R6 should be less than about 2 kcal/mol.

**MOVPE of $Cd_{1-y}Zn_yTe$.** Based on our previous studies of ZnTe MOVPE from DMZn and DIPTe, substantial zinc incorporation is expected for alloy growth from DMCd, DMZn, and DIPTe at 673 K.[12] However, from Figure 6a, it is apparent that the growth rate of ZnTe is zero for essentially all $x$ values except for the case where no DMCd is fed. Evidently, DMCd and DMZn compete for the same adsorption sites on the growth surface. The decomposition of DMCd seems to be energetically more favorable, thus inhibiting ZnTe growth. Similar observations were reported for $Cd_{1-y}Zn_ySe$ growth during photoassisted MOVPE.[25] Using DMCd, DMZn, and DESe, no zinc was incorporated into the film for any gas-phase zinc content less than 85%.

The metalorganic vapor-phase epitaxy of $Cd_{1-y}Zn_yTe$ alloys has been studied by Ahlgren et al.[8] and Kisker.[9] The organometallic compounds examined were DMCd, DEZn, and DETe. The ligand exchange reactions between the group II precursors account for the erratic zinc segregation observed by these researchers. We have found that ligand exchange in the feed influence the alloy growth in two distinct ways. First, the partial pressure of DEZn in the feed is lowered at the expense of the more stable exchange products, DMZn and MEZn. This trend is enhanced at temperatures exceeding 550 K (see Figure 5). This makes the incorporation of zinc below 720 K difficult, because little of the DEZn is left, and DMZn and MEZn do not decompose readily at those temperatures. In the case of DMZn, this is confirmed by the inability to grow the alloy using this precursor (see Figure 6a). Second, the DMCd is converted into the less stable products, DECd and MECd. For $x$ values greater than 0.6, there is virtually no DMCd left in the feed gas, and only MECd and DECd remain (see Figure 4). Since methylethylcadmium and diethylcadmium are thermally unstable, the incorporation of cadmium into the film is strongly favored. Consequently, near the reactor inlet, only pure CdTe is deposited in a thick layer, as seen in Figure 7.

Ahlgren and co-workers[8] observed that at 714 K the zinc preferentially incorporates into the film for all ratios of DMCd to DEZn in the gas inlet. At this substrate temperature, zinc incorporation may have been higher than in the present study, because more of the MEZn will have decomposed along with the DEZn. Nevertheless, the DMZn should still have been unreactive. Moreover, the gas flow velocities used in their study must have been very high to prevent the organocadmium compounds from reacting to form CdTe on the leading edge of the substrate. The use of high gas velocities is supported by their observation of an increasing zinc content over the length of the substrate, even though it was only 1 in. long. From the few details given of their growth conditions, we speculate that only a small amount of the cadmium but more of the zinc in the gas feed was available for film growth, hence the preferential incorporation of zinc in their films.

Kisker[9] obtained very different results. At 653 K, zinc was not incorporated in the film below $x = 0.3$, and nearly pure ZnTe was deposited when the vapor composition exceeds $x = 0.5$. This S-shaped zinc segregation behavior tends to stretch out and become more gradual as the growth temperature was raised to 673 K. Kisker also found a composition gradient over the length of the reactor. In spite of this, he chose to measure the composition at only one point in the system. Our observations of a strong gradient in the film composition with changing value of $x$ in Figure 7 helps to explain the S-shaped segregation behavior seen in Kisker's data. If the location in the reactor for film analysis had been closer to the inlet, then he would have observed a cadmium-rich film over the complete composition range of the gas phase. However, the location in the reactor chosen by Kisker for film analysis must have been at a point in the reactor, where the film composition can change suddenly with gas-phase composition from a cadmium-rich to a zinc-rich film. The exact location of this point in a horizontal reactor depends on the experimental conditions, such as temperature and flow rate.

Modeling of the $Cd_{1-y}Zn_yTe$ growth kinetics can be quite complicated with five reactive species in the feed (DMCd, MECd, DECd, DEZn, and DIPTe). Before the exchange reactions between the group II sources were discovered, we proposed a model for the growth of $Cd_{1-y}Zn_yTe$ that is based upon the following surface reaction mechanism: dissociative adsorption of the organometallic compounds, desorption of the alkyl ligands, film growth, and desorption of the excess zinc or cadmium metal.[10] This model predicted that the zinc segregation behavior would be relatively insensitive to the substrate temperature and the II/VI ratio. However, it would be strongly influenced by the intrinsic kinetic parameters, i.e., the difference in the cadmium and zinc sublimation energies and the relative sticking probabilities of the organometallic precursors.

The experimental results presented in Figure 8 are consistent with the trends predicted by the model. In spite of the large scatter of the data, it is evident that the distribution of zinc and cadmium between the phases is insensitive to the process conditions. According to our model, if the heats of sublimation of Cd and Zn are equal, then the alloy composition is determined by the relative adsorption rates of the group II compounds. This assumption is allowed in the present case because only cadmium sublimation is observed during MOVPE. The mole fraction of zinc in the solid phase, $y$, is given by (eq 36 in ref 10)

$$y = 1/(A + 1) \tag{12}$$

in which

$$A = \left(\frac{M_{\mathrm{DEZn}}}{M_{\mathrm{DRCd}}}\right)^{1/2} \frac{S_{\mathrm{DRCd}}}{S_{\mathrm{DEZn}}} \frac{1 - x}{x} \tag{13}$$

where $M$ and $S$ are the molecular weight (g/mol) and the initial sticking probability of the organometallic compound, and the subscript DRCd refers to the average value for the three reactive Cd sources, DMCd, MECd, and DECd. There is no need to consider MEZn and DMZn since they do not decompose appreciably under the reaction conditions studied. The solid curves shown in Figure 8 are the best fit of eq 12 to the data. This fit yields a ratio of the sticking probability of the cadmium compounds to diethylzinc, $S_{\mathrm{DRCd}}/S_{\mathrm{DEZn}}$, of 3.0. This ratio is consistent with the higher reactivity of the cadmium sources. The wide variation of data about the solid curve is due in part

to the uncertainty in the composition data and in part to the fact that the model does not account for variations in the concentrations of the reactants along the reactor. This latter problem could be solved by incorporating the model with differential mass balances for each reactant and then integrating these equations over the reactor length.

Alkyl ligand exchange of the group III organometallic precursors in III−V MOVPE has been reported by Grady et al.[26] They observed ligand exchange between trimethylamine alane and trimethylgallium to yield different gallane species and trimethylaluminum. The large difference in thermal stability between these compounds lead to nonuniformities in the composition of the $Al_xGa_{1-x}As$ films deposited in the MOVPE reactor. These results are consistent with our current investigation of $In_xGa_{1-x}As$ MOVPE. We have discovered that. even under low-pressure conditions, the group III precursors trimethylindium and triethylgallium exchange ligands and that this affects the segregation behavior of indium in the film.[27]

From the results presented in this study, we may conclude that growing $Cd_{0.96}Zn_{0.04}Te$ with $\Delta y = 0.001$ cannot be accomplished in a horizontal flow reactor because of the thorough upstream mixing of DMCd with DEZn. On the other hand, $Cd_{0.96}Zn_{0.04}Te$ has been successfully grown on GaAs/Si substrates at 523−553 K using a high-speed, rotating-disc reactor.[28−30] We suspect that in this reactor the DMCd and DEZn are fed through separate injection manifolds in the reactor headplate. This design, together with rapid mixing of the gases above the substrate, makes it possible to deposit alloy films of uniform composition over the entire substrate. Complex reactor designs of this type are essential when ligand exchange reactions of the sources leads to large differences in their thermal stability.

## Conclusions

We have discovered that ligand exchange reactions occur between the group II precursors during II−VI MOVPE. This appears to be a general phenomenon in the growth of II−VI and III−V alloys by this technique.[26,27] Although ligand exchange is well-documented in organometallic chemistry, its impact on the MOVPE process has not been widely recognized. With regard to $Cd_{1-y}Zn_yTe$ film growth, ligand exchange produces unstable cadmium compounds, DECd and MECd, and very stable zinc compounds, DMZn and MEZn. The large difference in reactivities of these sources makes it very difficult to uniformly incorporate controlled amounts of zinc into the alloy film over the entire area of the heated substrate.

**Acknowledgment.** The authors thank Dr. Kelvin Higa for useful discussion of the results. Funding for this research was provided by the Office of Naval Research (Award No. N00014-95-1-0904), the National Science Foundation, Solid-State Chemistry program (Grant No. DMR-9422602), and Chemical Thermal Systems program (Grant No. CTS-9531785). In addition, material in this study is based upon work supported by a National Science Foundation Graduate Fellowship to K.J.W. All of this support is greatly appreciated.

## References and Notes

(1) Dornhauf, R.; Nimtz, G. Narrow Gap Semiconductors. In Hohler, G. *Tracts in Modern Physics*; Springer: Berlin, 1983.
(2) Tung, J. *J. Cryst. Growth* **1988**, *86*, 161.
(3) Tennant, W. E.; Kozlowski, L. J.; Bubulac, L. O.; Gertner, E. R.; Vural, K. *IEEE Conf. Series* **1990**, *321*, 15.
(4) Filippozzi, J. L.; Therez, F.; Estève, D.; Fallahi, M.; Kendil, D.; da Silva, M.; Barbe, M.; Cohen-Solal, G. *J. Cryst. Growth* **1990**, *101*, 1013.
(5) Willardson, R. K., Beer, A. C., Eds. *Semiconductors and Semimetals*; Academic Press: New York, 1981; Vol. 18.
(6) Johnson, S. M.; Kalisher, M. H.; Ahlgren, W. L.; James, J. B.; Cockrum, C. A. *Appl. Phys. Lett.* **1990**, *56*, 946.
(7) de Lyon, T. J.; Johnson, S. M.; Cockrum, C. A.; Wu, O. K.; Hamilton, W. J.; Kamath, G. S. *J. Electrochem. Soc*. **1994**, *141*, 2888.
(8) Ahlgren, W. L.; Johnson, S. M.; Smith, E. J.; Ruth, R. P.; Johnston, B. C.; Kalisher, M. H.; Cockrum, C. A.; James, T. W.; Arney, D. L.; Ziegler, C. K.; Lick, W. *J. Vac. Sci. Technol. A* **1989**, *7*, 331.
(9) Kisker, D. W. *J. Cryst. Growth* **1989**, *98*, 127.
(10) Kappers, M. J.; McDaniel, A. H.; Hicks, R. F. *J. Cryst. Growth* **1996**, *160*, 310.
(11) McDaniel, A. H.; Wilkerson, K. J.; Hicks, R. F. *J. Phys. Chem.* **1995**, *99*, 3574.
(12) Wilkerson, K. J.; Kappers, M. J.; Hicks, R. F. *J. Phys. Chem.*, in press.
(13) Butler, I. S.; Newbury, M. L. *Spectrochim. Acta* **1977**, *33A*, 669.
(14) Kaesz, H. D.; Stone, F. G. A. *Spectrochim. Acta* **1959**, 360.
(15) Bellamy, L. J. *The Infra-red Spectra of Complex Molecules*; Wiley: New York, 1956.
(16) Jackson, J. A.; Nielson, R. J. *J. Mol. Spectrosc.* **1964**, *14*, 320.
(17) Cross, R. J.; Glockling, F. *J. Organomet. Chem.* **1965**, *3*, 146.
(18) Cullen, W. R.; Deacon, G. B.; Green, J. H. S. *Can. J. Chem.* **1966**, *44*, 717.
(19) Green, J. H. S.; Kynaston, W.; Rodley, G. A. *Spectrochim. Acta* **1968**, *24A*, 853.
(20) McCoy, C. R.; Allred, A. L. *J. Am. Chem. Soc.* **1962**, *84*, 912.
(21) Henold, K.; Soulati, J.; Oliver, J. P. *J. Am. Chem. Soc.* **1969**, *91*, 3171.
(22) Soulati, J.; Henold, K.; Oliver, J. P. *J. Am. Chem. Soc.* **1971**, *93*, 5694.
(23) Higa, K. T. Unpublished results.
(24) Pilcher, G.; Skinner, H. A. *The Chemistry of the Metal-Carbon Bond*; Wiley: New York, 1982.
(25) Bao, K. X.; Mo, R.; Kalisetty, S.; Gokhale, M.; Robinson, J.; Ayers, J. E.; Jain, F. C. Presented at the 8th International Conference on MOVPE, 1996.
(26) Grady, A. S.; Markwell, R. D.; Russell, D. K.; Jones, A. C. *J. Cryst. Growth* **1990**, *106*, 239.
(27) Kappers, M. J.; Warddrip, M. L.; Hicks, R. F. Manuscript in preparation.
(28) Tompa, G. S.; Salagaj, T; Cook, L.; Stall, R. A.; Nelson, C. R.; Anderson, P. L.; Wright, W. H.; Ahlgren, W. L.; Johnson, S. M. *J. Cryst. Growth* **1991**, *107*, 198.
(29) Johnson, S. M.; Vigil, J. A.; James, J. B.; Cockrum, C. A.; Cockrum, C. A.; Konkel, W. H.; Kalisher, M. H.; Risser, R. F.; Tung, T.; Hamilton, W. J.; Ahlgren, W. L.; Myrosznyk, J. M. *J. Electron Mater.* **1993**, *22*, 835.
(30) Anderson, P. L.; Erbil, A.; Nelson, C. R.; Tompa, G. S.; Moy, K. *J. Cryst. Growth* **1994**, *135*, 383.